AJBCPS African Journal of Biological, Chemical and Physical Sciences

Vol 4, Issue 1, 2025

ISSN: 2790-9522 (Print) | 2790-9530 (Online)
Website: https://journals.jozacpublishers.com/ajbcps/index

OPEN ACCESS

Moringa oleifera-derived copper oxide nanoparticles against plasmodium resistance

Stella Adedunni Emmanuel[1*], Omotola Michael Fayomi[2], Olutayo Olawumi Olajide[1]
[1]Chemistry Advanced Research Centre, Sheda Science and Technology Complex (SHESTCO), Abuja, Nigeria, sa.emmanuel@shestco.gov.ng
[2]Department of Chemistry, Joseph Sarwuan Tarka University, Makurdi. Nigeria.

*Correspondence: sa.emmanuel@shestco.gov.ng

Received: January 22, 2025 | **Accepted:** March 11, 2025 | **Published:** April 03, 2025

Abstract

The emergence of antimalarial drug resistance in Plasmodium species has necessitated the investigation of novel therapeutic interventions. This study reports the biosynthesis of copper oxide nanoparticles (CuO-NPs) mediated by Moringa oleifera (MO) stem bark and root extracts, designated as CuONPmose and CuONPmore, respectively. Comprehensive characterization of the synthesized nanoparticles was conducted using multiple analytical techniques: Scanning Electron Microscopy (SEM), UV-Visible spectroscopy (UV-Vis), Fourier Transform Infrared spectroscopy (FTIR), X-ray Diffraction (XRD), and Energy Dispersive X-ray spectroscopy (EDX). UV-Visible spectroscopic analysis revealed characteristic absorption maxima at 320 nm and 300 nm for the respective nanomaterials, confirming successful nanoparticle formation. FTIR spectroscopic analysis demonstrated Cu-O interactions at 678 cm−1, while the presence of carbonyl moieties at 1684 cm−1 indicated the involvement of plant-derived compounds as capping agents. Morphological examination via SEM revealed non-aggregated, spongy surface characteristics for both CuO-NPs. XRD and EDX analyses confirmed the formation of highly pure, crystalline nanostructures with average crystallite sizes of 12.46 nm and 10.66 nm for CuONPmose and CuONPmore, respectively. In vivo assessment of anti-plasmodial efficacy demonstrated moderate inhibitory activity against P. berghei proliferation. The synthesized CuO-NPs exhibited superior parasitemia suppression compared to the crude M. oleifera stem bark and root extracts, suggesting enhanced therapeutic potential of the nanoformulations.

Keywords: Copper nanoparticles, Moringa oleifera, Plasmodium resistance, Root extract, Stem bark

1. Introduction

Plasmodium resistance in malaria treatment has triggered a global concern, particularly with the emerging resistance of a standard drug like artemisinin (Yasri & Wiwanitkit, 2021). This resistance challenges the accomplishments gained in decreasing malaria fatality rates and may hamper control efforts, especially in Sub-Saharan Africa (Sundararaman & Odom John, 2022). The concern is further

heightened by the limitation to examine the resistance of the causal *Plasmodium* species through an *in vitro* assay (Asih & Syafruddin, 2016).

To solve these issues, nanomaterials, because of their biocompatibility and minimal toxicity, are fabricated to release drugs to active sites for malaria treatment, making them an enticing alternative to traditional treatment (Kekani & Witika, 2023). It is critical to continuously study novel alternatives for the treatment of malaria and its attending Plasmodium resistance as observed with the current treatment regime. Despite several reports on nanomaterials being researched for antimalarial drug resistance, there is still an opportunity for additional compounds.

2. Literature review

While existing studies have unveiled promising candidates, such as metal oxide nanoparticles (Alprol et al., 2023). Among others, the efforts in this work focus on finding novel drugs with anti-parasitic activity, though not minding their mechanisms of action and possibly challenges relating to toxicity and biocompatibility. Literature revealed reports on varieties of metal oxide nanoparticles prepared by the use of extracts from natural sources such as plant materials. For instance, nanoparticles of copper synthesized using *MO* leaf extract, exhibited some bioactivities like high antioxidant, cytotoxic (Rehana et al., 2017) and antimicrobial (Das et al., 2020) activities. This synthetic route involving the composition of a plant in solution is eco-friendly, cost-effective, and provides a suitable alternative to traditional chemical methods (Yedurkar et al., 2020).

Moringa oleifera is a plant with a range of bioactive compounds. The extract of this plant contains tannins, saponins, cardiac glycosides, terpenes, steroids, flavonoids, and alkaloids (Etejere et al., 2017). These bioactive compounds cause reduction and stabilization to produce copper oxide nanoparticles. These natural capping and reductants in the plant increase the conversion of copper ions into nanoparticles while avoiding agglomeration (Khaldari et al., 2021). Regardless of the part of the Plant, scientists have utilized the fruit, leaf, stem, and root parts to synthesize metal oxide nanoparticles (Chakraborty et al., 2022).

Specifically, aqueous extract obtained from *Solanum macrocarpon* fruit has been used to synthesize copper oxide nanoparticles (Okpara et al., 2021). The root extract of *Ixora coccinea* (Yedurkar et al., 2020), and extracts from the stem of *Sarcostemma acidum* have been used to derive copper nanoparticles, respectively (Roseline & Priya, 2023). The efficacy of copper oxide (CuO) nanoparticles obtained from stem or root extract compared to those from leaf extract has been attributed to the distinct phyto-composition of these plant parts (Okpara et al., 2021). The plant extract produces electrons to reduce copper salts. Copper oxide nanoparticles are designed as a result of the reaction between the plant's phytochemicals and copper ions (Sharma et al., 2018). The bioactive compounds present in plant material are easily degradable, thereby affecting the size and nature of the nanoparticles formed. Also, the temperature of preparation and other conditions can influence the size and properties of the nanoparticles (Luque-Jacobo et al., 2023).

Therefore, the specific phytochemical composition in stem and root extracts, as well as the synthesis conditions, may lead to the production of copper oxide nanoparticles with enhanced

efficacy compared to those derived from leaf extracts (Naz et al., 2023). Green synthesis of CuO nanoparticles with stem and root extract of plants is an area of active research, and it holds promise for the development of novel nanomaterials with tailored properties. The use of plant materials in the preparation of nanoparticles not only contributes to the sustainable utilization of natural resources but also leads to the production of nanoparticles with potential applications in diverse areas, including catalysis, sensing, and healthcare. Therefore, the role of plants in green synthesis cannot be overemphasized, offering a sustainable and environmentally friendly approach to nanomaterial production with wide-ranging potential applications (Bhavyasree & Xavier, 2022).

The use of green-synthesized copper oxide nanoparticles obtained from plant stem and root has been found to be more effective in combating malaria than plant extracts alone (Tadesse & Guesh, 2024). The eco-friendly nature of the synthesis process and the improved properties of the synthesized nanoparticles make this approach promising for the development of sustainable and effective antimalarial treatments (Gujjari et al., 2022; Shehab et al., 2024). Recent studies have shown CuO nanoparticles exhibit significant anti-malarial action against Plasmodium falciparum, (Jayaseelan et al., 2022). This work was aimed at synthesizing the copper nanoparticles from the *MO* stem and root extracts, as well as further deducing their anti-plasmodial properties.

3. Research methodology

3.1. Preparation of *MO* Stem Bark and Root Extracts

Fresh samples of *MO* stem bark and root were harvested from the Medicinal Garden at Sheda Science and Technology Complex (SHESTCO), Abuja. Both samples were washed, air dried, and pulverized with a laboratory blender. 6 g of fine powder of each part was weighed, added to 200 mL deionized water in a 500 mL beaker, and heated at 100 °C for about 30 minutes, respectively. The extract from each sample, denoted MOSE for stem bark extract and MORE for root extract, was filtered using filter paper (Whatman no. 1) and stored at 4°C for further use.

3.2. Synthesis of CuO Nanoparticles with MOSE and MORE

Copper acetate (0.02 M) in 70 mL of deionized water was mixed with 30 mL of *MOSE* extract along with 0.2 M of NaOH solution which was added dropwise. A homogeneous solution was formed on stirring at 70 ^{o}C for 2 hours to give a green precipitate on settling. The product (copper oxide nanoparticles) was collected by centrifugation and washed severally with ethanol/water mixture. The product was oven dried at 90^{o}C for 3 hours, and then calcined in a pre-heated muffle furnace at 400 ±10^{o} C to give a brown coloured solid (Rehana et al., 2017). The synthesized CuO nanoparticles were denoted as CuONPmose and CuONPmore, indicating stem and root extracts, respectively.

3.3. Characterization of study nanoformulations

The characterization of both CuONPmose and CuONPmore utilized some analytical techniques. UV–Vis absorption spectroscopy was carried out via a JENWAY 6405 UV-Vis spectrophotometer to confirm and elucidate the synthesis. The spectra of the nanoparticles were obtained through a wavelength scan spanning from 200 to 800 nm. The information from the UV-Vis spectra indicates the reduction of copper ions in the synthesis and the completion of the reaction. The Fourier

Transform Infra-Red FT-IR spectra of nanomaterials were recorded using an Agilent 630 Cary FT-IR Spectrophotometer equipped with both ATR and 'Dial Path' modules for versatile analysis of liquids, solids, films, and gels. CuONPmose and CuONPmore samples were prepared on KBr discs using a 4% (w/w) solid/KBr mixture, and FT-IR spectra were acquired in the range of 400–4,000 cm^{-1}. This technique provided insights into bond details and molecular composition of the materials.

For structural characterization, X-ray Diffraction (XRD) analysis was conducted on the two copper oxide nanomaterials using a Thermo Scientific model ARL 'XTRA X-ray instrument. This non-destructive method provides evidence on assemblies, phases, texture, lattice parameters, chemical composition, as well as parameters like grain size, crystallinity, strain, and crystal defects. Surface morphology and structural analysis were further explored through SEM/EDX (Scanning Electron Microscopy/Electron Dispersive X-ray) using a Phenom World model PRO:X:800-07334. This technique provided detailed information on surface features, pore structure, and particle size analysis, particularly beneficial for nanoparticle materials. These analytical approaches give extensive insights into the synthesis and structural properties of CuONPs.

3.4. Experimental Animal studies

The Wistar rats used in the experiment were obtained from the College of Veterinary Medicine at Joseph Sarwuan Tarka University in Makurdi. These rats were grouped and housed in individual 15x30cm cages with metal tops and kept clean. Wood shavings (sawdust) were used as bedding materials and replenished on a weekly basis to guarantee the animals' cleanliness and to prepare them for work.

3.5. *In vivo* Parasitaemia Infection Assessment

CuONPmose and CuONPmore, along with their respective crude extracts, were verified against plasmodial resistance adapting a methodology previously reported (Gitau et al., 2023). The experimental wistar rats of 115 – 120 g weight were meticulously selected and underwent a period of acclimatization spanning 2 weeks, ensuring their physiological equilibrium prior to experimentation. Subsequently, these animals were randomly partitioned into six distinct groups, each comprising a pair of rats. Groups 1-4 were earmarked as the experimental cohorts, with two receiving CuONPmose and CuONPmore while the other two were administered crude extracts. In parallel, group 5 was designated positive control, receiving the established antimalarial drug Artemether, while group 6 remained untreated to serve as negative control, allowing for comparison against the treated groups. To initiate the infection model, approximately 2 mL of freshly drawn blood from the rats was meticulously mixed with 0.6 mL of normal saline. Subsequently, the rats were induced with 0.5 mL of parasitaemia (1×10^7 Plasmodium berghei) intraperitoneally, facilitating the establishment of the Plasmodium parasite within their system. This crucial incubation period spanned 24 hours, allowing for the proliferation and spread of the parasite throughout the host.

After this phase, the designated treatments were administered to their respective groups, maintaining a standardized dosage of 50 mg/kg body weight for each agent. These treatments were left to exert their effects for 48 hours, enabling an assessment of their activity. Post-treatment, blood samples were diligently collected from the tail of each rat and smeared onto clean glass slides,

forming thin blood films. These slides underwent air-drying, fixation with methanol, staining with Giemsa stain for 10 minutes, and subsequent rinsing. The prepared slides were then scrutinized under a high-powered microscope equipped with a x100 objective lens. The assessment parameters, namely percentage parasitemia and percentage inhibition on the red blood cells (RBC), were calculated utilizing established equations (1) and (2). This experimental design is aimed at explaining the relationship between the test agents and their efficacy against the plasmodium parasite, potentially offering insights into combating malaria resistance.

$$\% \text{ Parasitaemia} = \frac{Number\ of\ Parasitized\ Cells\ x\ 100}{Number\ of\ Red\ Blood\ Cells\ (RBC)} \quad (1)$$

$$\% \text{ Inhibition} = \frac{\%\ Parasitaemia_{control} - \%\ Parasitaemia_{test\ group}\ x\ 100}{\%\ Parasitaemia_{control}} \quad (2)$$

4. Data analysis

The data generated from the experiment were analyzed using OriginPro Software® 2017, a robust analytical tool renowned for its precision and versatility. One-way Analysis of Variance served as a primary tool for comparing means across multiple groups, followed by post-hoc tests utilizing the Tukey and Levene methods. These post-hoc analyses allowed for the identification of specific group differences and the determination of the homogeneity of variances, ensuring the robustness and validity of the findings. The findings of the study were presented as mean value accompanied by the standard deviation of the mean (M±SD), providing a comprehensive insight into the central tendency and variability of the data. Throughout the analysis, differences were deemed statistically significant if the p-value was less than 0.05, signifying a high-level confidence in the observed effects.

5. Results and discussions

Characterization of CuONPs

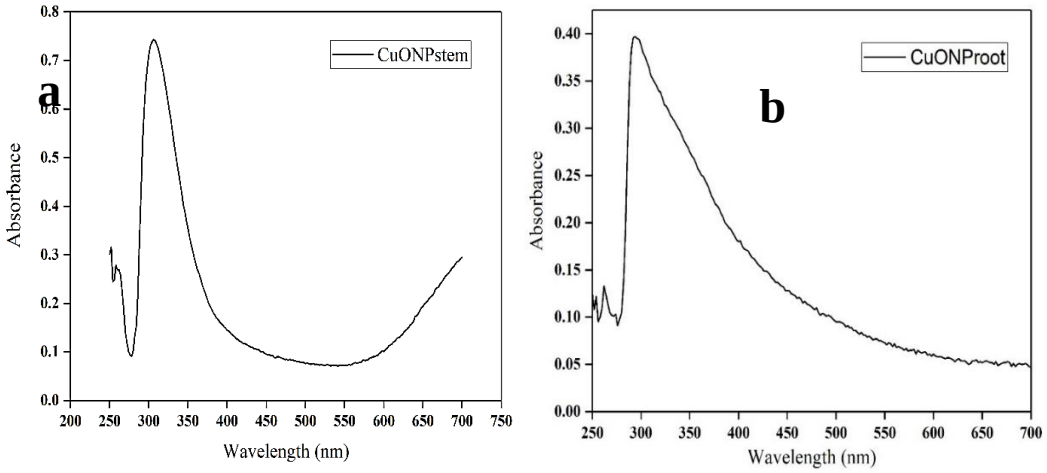

Figure 1: UV-Visible Spectra of (a). CuONPmose (b). CuONPmore

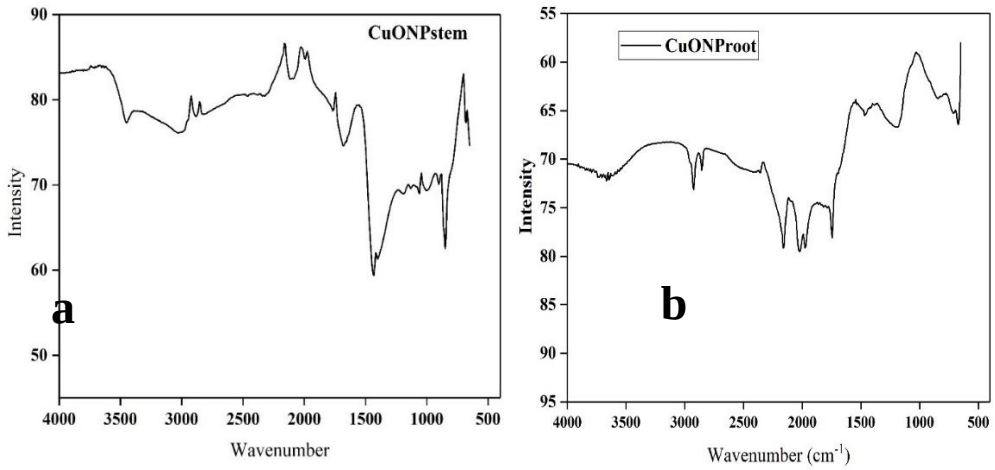

Figure 2: FTIR spectra of (a). CuONPmose and (b). CuONPmore

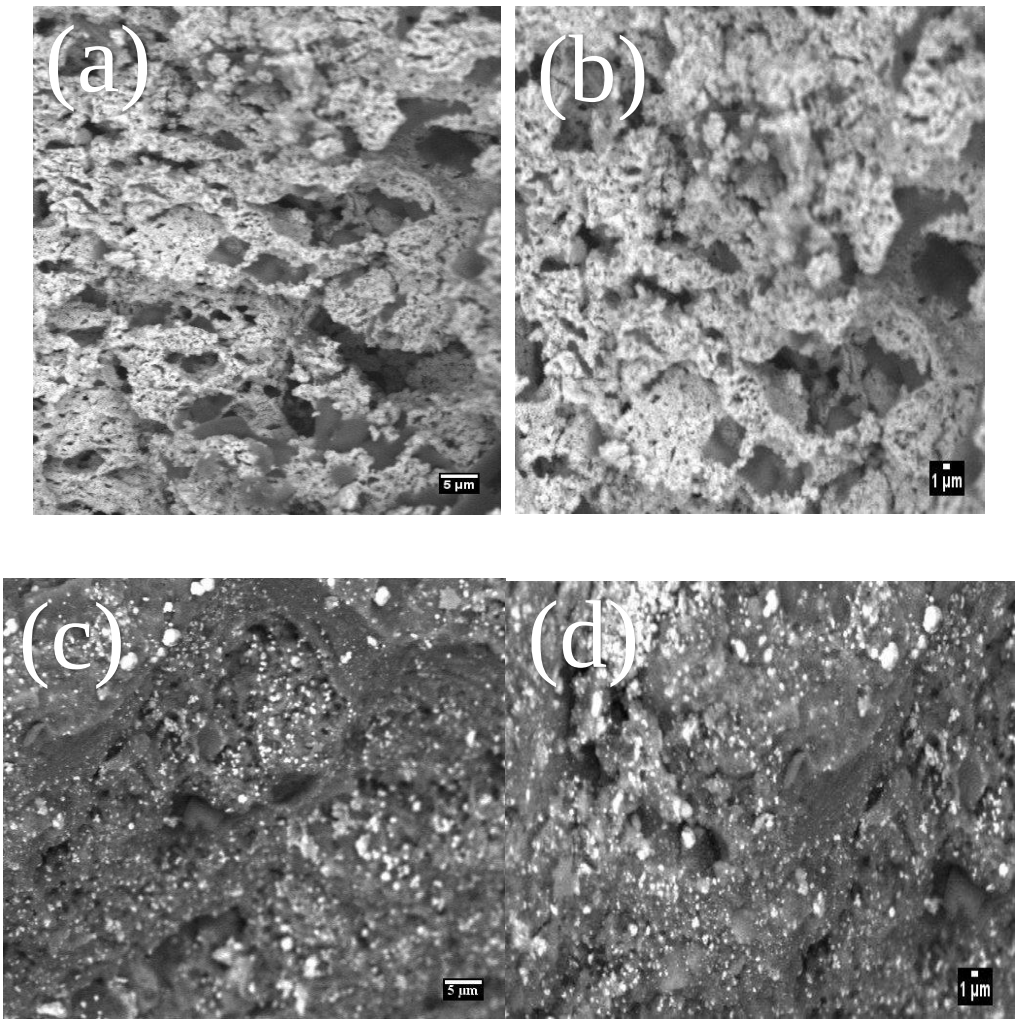

Figure 3: SEM images of (a) CuONPmose (5µm) (b) CuONPmose (1 µm) (c) CuONPmore (5µm) (d) CuONPmore (1 µm)

Table 1: EDX Weight Ratio of Electrospun CuONPmose and CuONPmore

		CuONPmose (a)		CuONPmore (b)	
Element Number	**Element Name**	**Atomic Conc.**	**Weight Conc.**	**Atomic Conc.**	**Weight Conc.**
29	Copper	57.71	78.33	64.88	80.67
11	Sodium	37.62	18.47	9.14	4.11

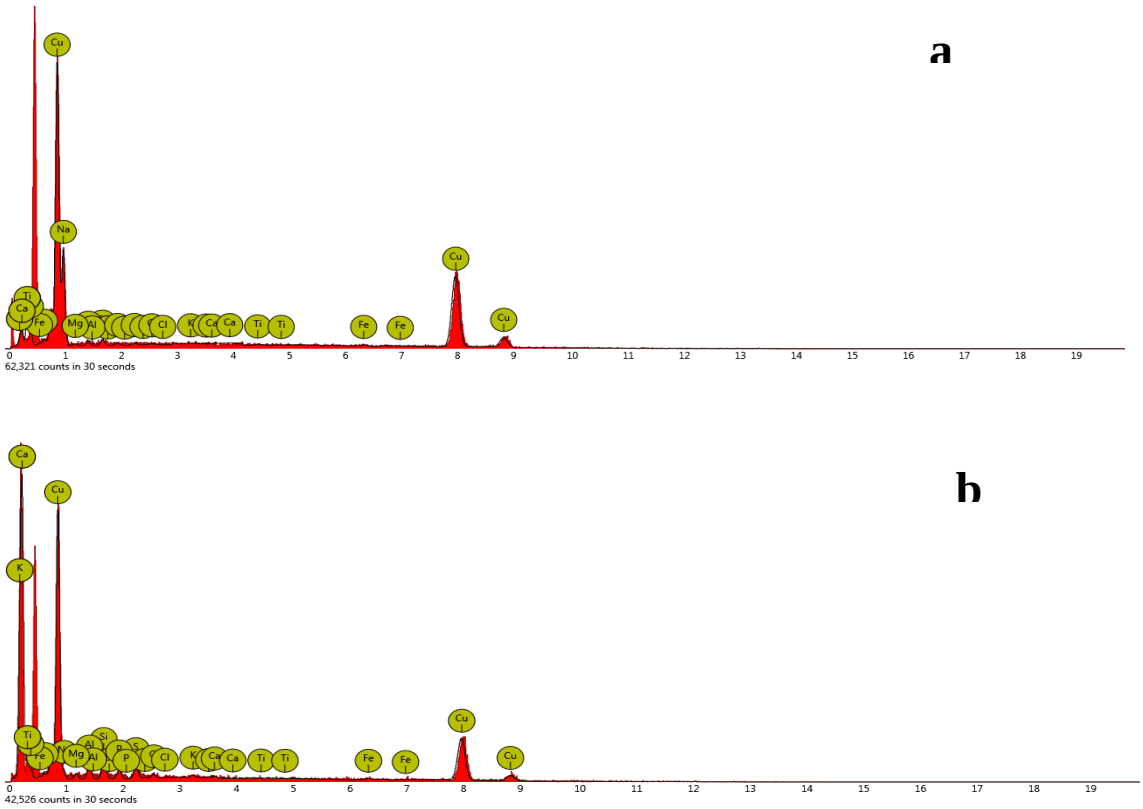

Figure 4: EDX of (a). CuONPmose (b). CuONPmore showing the elemental composition of the nanopaticles

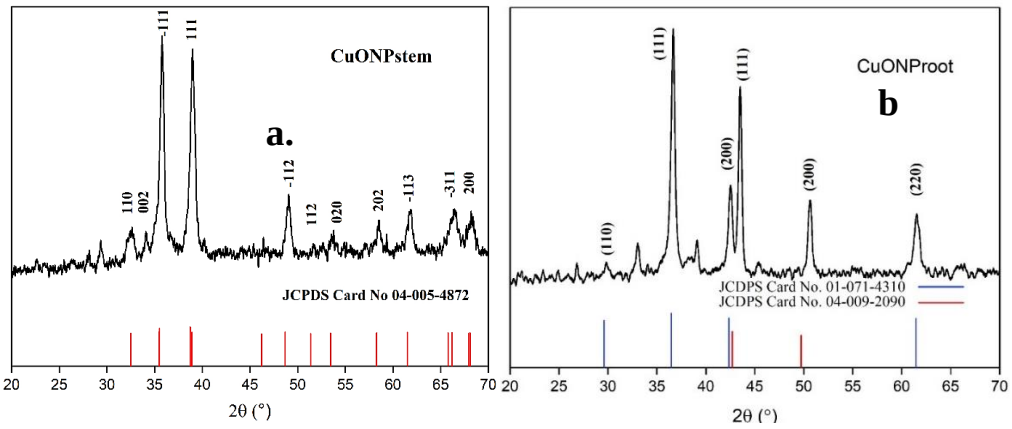

Figure 5: XRD patterns showing different peak positions at 2θ along with the JCPDS card number indicating the miller indices of (a). CuONPmose and (b). CuONPmore.

Table 2: Some Crystallographic Parameters of the Synthesized CuONPs derived from *M. Oleifera* Stem Bark Extract based on the X-Ray Diffraction Pattern.

S/N	Peak Position (2θ)	FWHW (β) (degree)	Crystallite size D (nm)	D (Average) (nm)
1	29.82	1.0574	7.77	12.46
2	33.04	0.6499	12.75	
3	36.68	0.4906	17.06	
4	39.12	1.1319	7.45	
5	42.52	0.5983	14.25	
6	43.52	0.4398	19.45	
7	45.40	1.5465	5.57	
8	50.62	0.5288	16.62	
9	61.54	0.8247	11.21	

Table 3: Some Crystallographic Parameters of the Synthesized CuONPs derived from *M. oleifera* Root Extract based on the X-Ray Diffraction Pattern

S/N	Peak Position (2θ)	FWHW (β) (degree)	Crystallite size D (nm)	D (Average) (nm)
1	29.86	0.6483	12.2556	10.66
2	36.66	1.2067	6.5835	
3	42.56	0.9250	8.5888	
4	43.52	0.5420	14.6570	
5	50.64	0.6733	11.7991	
6	61.54	0.7896	10.0616	

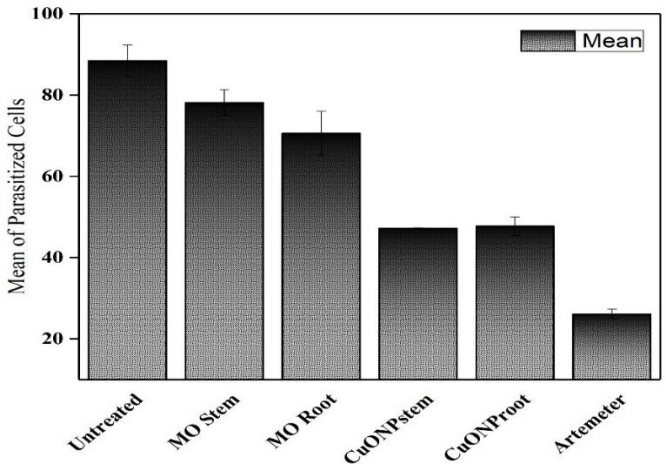

Figure 6: Number of Parasitized Cells of the Negative Control and Test Groups of Wistar Rats

Table 4: Antiplasmodial Activity of *MO* Extracts and derived CuO Nanoparticles

Samples	Negative Control	*MOSE*	*MORE*	CuONPmose	CuONPmore	Artemether
% Inhibition on the Parasites	0	11.36 ± 7.39	20.30± 2.63	46.54±2.15	46.06±0.22	70.45±0.00

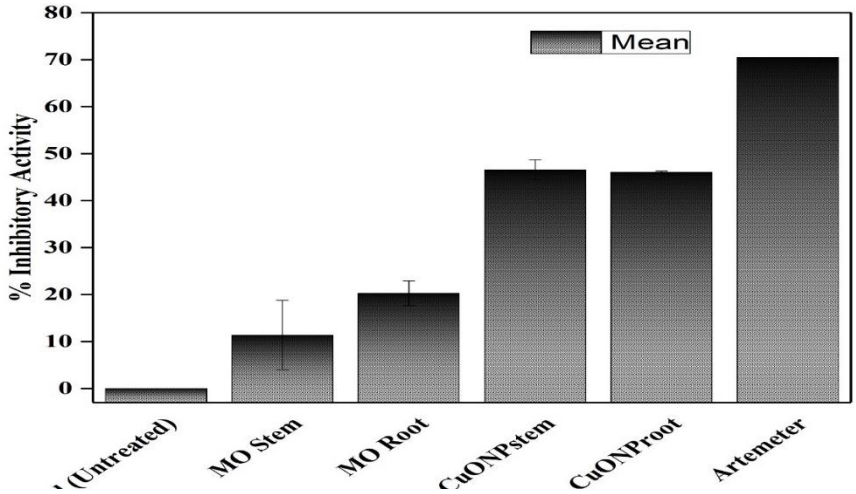

Figure 7: *In vivo* Anti-plasmodial Activity in percentage of *MO Stem Bark, Root* Extracts and CuO Nanoparticles

UV–Vis analysis

The characterization of CuONPmose and CuONPmore, through UV-Vis analysis presents insights into the structural characteristics of the synthesized material. Figures 1(a and b), show the spectra of the nanomaterials through the wavelength range of 250-700 nm, with a prominent peak observed around 320 nm and 300 nm, this suggests a successful formation of CuONPmose and CuONPmore. The presence of these distinct peaks indicates the absorption of electromagnetic radiation in ultra-violent region by the synthesized CuO nanoparticles (Aaga & Anshebo, 2023).

FT-IR Result

The FTIR spectra of the two nanoparticles in Figures 2 (a and b) further provide valuable insights into their structural and chemical properties. The vibrational frequencies of CuONPmose in Figure 2a showed prominent peaks at 678 cm^{-1}, 849 cm^{-1}, 1059 cm^{-1}, 1192 cm^{-1}, 1431 cm^{-1}, 1684 cm^{-1}, 2832 cm^{-1}, 2885 cm^{-1}, 3027 cm^{-1}, and 3452 cm^{-1}, while CuONPmore in figure 2b showed peaks at 775 cm^{-1}, 1029 cm^{-1}, 1364 cm^{-1}, 1543 cm^{-1}, and 3116 cm^{-1}. These peaks correspond to specific vibrational modes in the samples and can be attributed to various chemical bonds and functional groups present within the nanoparticles (Matei et al., 2023). For instance, the peak at 678 cm^{-1} may indicate the presence of Cu-O stretching vibrations, while peaks at higher wavenumbers like 1684 cm^{-1} could be associated with C=O stretching vibrations, suggesting the presence of bioactive compounds in the plant which served as respective capping agents. Additionally, the broad absorption peak at around 3452 cm^{-1} in the spectrum is attributed to adsorbed water molecules, which is common in nanostructured

materials due to their high surface area (Akpomie & Conradie, 2023). The absence of some peaks observed in CuONPmose, such as those at 2832 cm^{-1} and 3452 cm^{-1}, and the presence of unique peaks in CuONPmore, such as the one at 3116 cm^{-1}, indicate distinct chemical environments or bonding configurations in the two copper oxide nanoparticles (Radhakrishnan & Beena, 2014).

Common peaks in both spectra likely denote fundamental characteristics inherent to copper oxide nanoparticles. Conversely, disparities in peak locations or strengths imply alterations in nanoparticle structure, elucidating the interactions between copper ions and the components differently present in both parts of *Moringa oleifera*. Moreover, additional techniques such as XRD or SEM further complement the FTIR analysis, providing explanations into the crystalline structure and morphology of the nanoparticles (Mohamed, 2020).

Morphology of synthesize CuONPs

The SEM examination showed the surface images for both CuONPmose and CuONPmore (Teklu et al., 2023). The images for the CuONPs revealed fascinating images, as shown in figures 3a-d for their respective 5μm and 1 μm magnifications. CuONPmose showed spongy images; there also appeared some irregular spherical hollows on the surfaces of the two copper oxide nanoparticles (Ali et al., 2023).

Composition of synthesized CuONPs

Energy Dispersive X-ray Spectroscopy (EDX) is used to analyze the elemental constitution of materials, including copper oxide nanoparticles. The EDX result revealed the amount of copper and oxygen as well as other elements within synthesized nanoparticles, thereby giving needed insights into their composition and purity (Kumar et al., 2022). The analysis of CuONPmose (Table 1, column a) shows atomic concentrations comprising 57.71% copper, alongside weight concentrations encompassing 37.62% copper (Prakash et al., 2023). While in column b, the result of CuONPmore revealed atomic concentrations of 64.88% copper, with weight concentrations delineating 9.14% copper (Gamedze et al., 2022). These findings, as they appear in figures 4a and b, indicate that CuO nanoparticles derived from root extract boast a greater copper abundance.

XRD Pattern of CuONPs

The Powder XRD pattern of the synthesized CuONPmose (Figure 5a) showed diffraction peaks that can be indexed to tenorite of CuO (JCPDS card number 04-005-4872). The diffraction peaks observed at 2θ values of 29.82°, 33.04°, 36.68°, 39.12°, 42.52°, 43.52°, 45.40°, 50.62°, and 61.54°, corresponding to the crystal planes of (110), (002), (111), (111), (-112), (112), (020), (020), (202), (-113), (-311), and (220) respectively. The values presented in Table 2 indicated calculated crystallite size ranging from 7.45 nm to 19.45 nm, with an average size of 12.46 nm. The crystallinity of CuONPmose is 57.91, indicating the presence of small nanocrystals. While the Powder XRD pattern of CuONPmore (Figure 5b) presents diffraction peaks that can be indexed as Cuprite of JCPDS Card number 01-071-4310 and Copper of JCDPS Card number 04-009-2090. The diffraction peaks observed at 2θ values of 29.86°,

36.66°, 42.56°, 50.64°, and 61.54° corresponding to the crystal planes of (110), (111), (200), (111), (200), and (220), respectively. The calculated crystallite size for CuONPmore ranges from 6.58 nm to 14.66 nm as shown in Table 3, with an average size of 10.66 nm. The crystallinity of CuONProot is 56.94, indicating the presence of relatively larger nanocrystals (Luna et al., 2015; Selvaraj, 2022).

The XRD patterns and EDX spectra suggested that the prepared CuO-NPs were pure, crystalline, and nano-sized. In addition to the diffraction peaks and crystal planes, the values of full width half maximum (FWHM, β), crystallite size (D), and related conversions are presented in Tables 2 and 3. The coherent volume in a material for the respective diffraction peak is referred to as the crystallite size. For a powdered material, it also corresponds to the grain size, and for polycrystalline thin films, it corresponds to the thickness. Therefore, calculating the crystallite size of this synthesized CuONPs, the Scherrer equation (3) is used.

$$D = \frac{K\lambda}{\beta \cos\theta} \quad (3)$$

In the equation (3), D is the crystallite size (nm), K= 0.9 is the Scherrer constant (also referred to as shape constant), λ is the wavelength of the X-ray source used to strike the crystal (0.15406 nm), β is the full width at half maximum (FWHM) of the diffraction peak used for the calculation (radians), and θ is the peak position (radians) (Selvaraj, 2022).

$$\text{Crystallinity} = \frac{Area\ of\ crystalline\ peaks}{Area\ of\ all\ peaks\ (crystalline+amorphous)}\ x\ 100 \quad (4)$$

Antiplasmodial Evaluation of synthesized CuONPs

The assessment of in vivo anti-plasmodial efficacy involved determining the percentage inhibition of the test samples against *P. berghei* growth. Results demonstrated a moderate activity for CuONPs against *P. berghei* growth, along with active inhibition of parasitemia. Figure 6 presents the mean parasitized cell counts of both negative control and test groups in experimental Winstar rats, with values expressed as mean ± standard error, with significance set at $p < 0.05$ for comparison. Figure 7 illustrates inhibitory activities of CuONPmose and CuONPmore against parasitemia, with values in the range of 46.54 ± 2.15 and 46.06 ± 0.22, respectively, compared to their corresponding crude extracts MOSE (11.36 ± 7.39) and MORE (20.30 ± 2.63). Notably, the positive control, Artemether, displayed the highest inhibition value of 70.45 ± 0.00, as detailed in Table 4 (Jayaseelan et al., 2022).

The use of CuONPs in inhibiting the growth of *P. berghei* and parasitemia is a novel approach with potential applications for the control of malaria. These results contribute to the growth of the literature on the use of nanomaterials for the management of parasitic diseases, including malaria (Bajwa et al., 2022).

6. Contribution of research to knowledge

Studies have shown that nanoparticles exhibit significant anti-malarial action against Plasmodium falciparum. The results of copper nanoparticles from the *MO* stem and root extracts give additional information on the anti-plasmodial properties of nanomaterials derived from plants and their

potential use in malaria therapy. It also showed that the Metal oxide nanoparticles have improved activities against the parent plant extract.

Moringa Oleifera is known for its ayurveda medicinal application, derivatizing its various parts' extract with metal oxide has the potential to improve its medicinal properties, as shown in this study. Further studies on metal oxides nanoparticles of the plant's extract with metals such as Zn and Ag are recommended.

7. Conclusion

The CuO nanoparticles synthesized using *MOSE* and MORE showed moderate activity against *P. berghei* growth and active inhibition of parasitemia. The nanoparticles were characterized using various techniques, including UV-VIS, FTIR, SEM, EDX and XRD. The assessment of *in vivo* anti-plasmodial efficacy involved determining the percentage inhibition of the test samples (the copper nanoparticles and their corresponding plant extract) against *P. berghei* growth. The results showed that CuONPmose and CuONPmore exhibited a higher inhibition value compared to their corresponding *M. Oleifera* Stem Bark Extract and *M. Oleifera* Root Extract.

ORCID

Stella Adedunni Emmanuel https://orcid.org/0000-0001-9392-666X
Omotola Michael Fayomi https://orcid.org/0000-0001-7971-605X
Olutayo Olawumi Olajide https://orcid.org/0000-0001-9615-4183

References

1. Aaga, G. F., & Anshebo, S. T. (2023). Green synthesis of highly efficient and stable copper oxide nanoparticles using an aqueous seed extract of Moringa stenopetala for sunlight-assisted catalytic degradation of Congo red and alizarin red s. *Heliyon*, *9*(5), e16067.
2. Akpomie, K. G., & Conradie, J. (2023). Efficient adsorptive removal of paracetamol and thiazolyl blue from polluted water onto biosynthesized copper oxide nanoparticles. *Scientific Reports*, *0123456789*, 1–15.
3. Ali, S. G., Haseen, U., Jalal, M., Khan, R. A., Alsalme, A., Ahmad, H., & Khan, H. M. (2023). Green Synthesis of Copper Oxide Nanoparticles from the Leaves of Aegle marmelos and Their Antimicrobial Activity and Photocatalytic Activities. *Molecules*, *28*(22).
4. Alprol, A. E., Mansour, A. T., Abdelwahab, A. M., & Ashour, M. (2023). Advances in Green Synthesis of Metal Oxide Nanoparticles by Marine Algae for Wastewater Treatment by Adsorption and Photocatalysis Techniques. *Catalysts*, *13*(5).
5. Asih, P. B. S., & Syafruddin, D. (2016). Plasmodium vivax and Drug Resistance. *IntechOpen*, *11*(tourism), 13.
6. Bajwa, H. U. R., Khan, M. K., Abbas, Z., Riaz, R., Rehman, T. U., Abbas, R. Z., Aleem, M. T., Abbas, A., Almutairi, M. M., Alshammari, F. A., Alraey, Y., & Alouffi, A. (2022). Nanoparticles: Synthesis and Their Role as Potential Drug Candidates for the Treatment of Parasitic Diseases. *Life*, *12*(5), 1–16.

7. Bhavyasree, P. G., & Xavier, T. S. (2022). Green synthesised copper and copper oxide based nanomaterials using plant extracts and their application in antimicrobial activity: Review. *Current Research in Green and Sustainable Chemistry*, *5*(December 2021), 100249.

8. Chakraborty, N., Banerjee, J., Chakraborty, P., Banerjee, A., Chanda, S., Ray, K., Acharya, K., & Sarkar, J. (2022). Green synthesis of copper/copper oxide nanoparticles and their applications: a review. *Green Chemistry Letters and Reviews*, *15*(1), 185–213.

9. Das, P. E., Abu-Yousef, I. A., Majdalawieh, A. F., Narasimhan, S., & Poltronieri, P. (2020). Green Synthesis of Encapsulated Copper Nanoparticles Using a Hydroalcoholic Extract of Moringa oleifera Leaves and Assessment of Their Antioxidant and Antimicrobial Activities. *Molecules*, *25*(3).

10. Etejere, E. O., Olayinka, B. U., & Lawal, L. O. (2017). Comparative studies of phytochemical constituents of leaf , bark and root of Moringa oleifera Lam. *Jewel Journal Science Reaserch. 3(1)*, *January 2015*, 173–176.

11. Gamedze, N. P., Mthiyane, D. M. N., Babalola, O. O., Singh, M., & Onwudiwe, D. C. (2022). Physico-chemical characteristics and cytotoxicity evaluation of CuO and TiO2 nanoparticles biosynthesized using extracts of Mucuna pruriens utilis seeds. *Heliyon*, *8*(8), e10187.

12. Gitau, W., Edinah, Kwamboka Songoro Jeremiah, Waweru Gathirwa Francis, K., & Kariuki, H. N. (2023). In vivo antiplasmodial activities of stem bark extracts of Avicennia marina in Plasmodium berghei -infected mice. *Pan African Medical Journal*, *44*(93), 1–19.

13. Gujjari, L., Kalani, H., Pindiprolu, S. K., Arakareddy, B. P., & Yadagiri, G. (2022). Current challenges and nanotechnology-based pharmaceutical strategies for the treatment and control of malaria. *Parasite Epidemiology and Control*, *17*(December 2021), e00244.

14. Jayaseelan, C., Abdulhaq, A., Ragavendran, C., & Mohan, S. (2022). Phytoconstituents Assisted Biofabrication of Copper Oxide Nanoparticles and Their Antiplasmodial, and Antilarval Efficacy: A Novel Approach for the Control of Parasites. *Molecules*, *27*(23).

15. Kekani, L. N., & Witika, B. A. (2023). Current advances in nanodrug delivery systems for malaria prevention and treatment. In *Discover Nano* (Vol. 18). Springer US.

16. Khaldari, I., Naghavi, M. R., & Motamedi, E. (2021). Synthesis of green and pure copper oxide nanoparticles using two plant resources: via solid-state route and their phytotoxicity assessment. *RSC Advances*, *11*(6), 3346–3353.

17. Kumar, D., Shukla, H., & Sharma, N. (2022). Antibacterial and morphological studies of plant-mediated synthesized CuO nanoparticles using Azadirachta indica (neem) leaf extract. *International Journal of Nano Dimension*, *13*(2), 197–204.

18. Luna, I. Z., Hilary, L. N., Chowdhury, A. M. S., Gafur, M. A., Khan, N., & Khan, R. A. (2015). Preparation and Characterization of Copper Oxide Nanoparticles Synthesized via Chemical Precipitation Method. *OALib*, *02*(03), 1–8.

19. Luque-Jacobo, C. M., Cespedes-Loayza, A. L., Echegaray-Ugarte, T. S., Cruz-Loayza, J. L., Cruz, I., de Carvalho, J. C., & Goyzueta-Mamani, L. D. (2023). Biogenic Synthesis of Copper Nanoparticles: A Systematic Review of Their Features and Main Applications. *Molecules*, *28*(12).

20. Matei, A., Craciun, G., Romanitan, C., Pachiu, C., and Tucureanu, V. (2023). *Biosynthesis & Characterization of Copper Oxide Nanoparticles*. 54. 14629

21. Mohamed, E. A. (2020). Green synthesis of copper and copper oxide nanoparticles using the extract of seedless dates. *Heliyon*, *6*(1), e03123.

22. Naz, S., Gul, A., Zia, M., & Javed, R. (2023). Synthesis, biomedical applications, and toxicity of CuO nanoparticles. *Applied Microbiology and Biotechnology*, *107*(4), 1039–1061.

23. Okpara, E. C., Ogunjinmi, O. E., Oyewo, O. A., Fayemi, O. E., & Onwudiwe, D. C. (2021). Green synthesis of copper oxide nanoparticles using extracts of Solanum macrocarpon fruit and their redox responses on SPAu electrode. *Heliyon*, *7*(12), e08571.

24. Prakash, M. V. D., Sampath, S., Amudha, K., Nadeem, A., Lopes, B. S., Durga, B., & Muthupandian, S. (2023). Eco-friendly green synthesis of copper nanoparticles from Tinospora cordifolia leaves: optical properties with biological evaluation of anti-microbial, anti-inflammatory and anti-oxidant applications. *Materials Technology*, *38*(1), 1–13.

25. Radhakrishnan, A. A., and Beena, B. B. (2014). Structural & Optical Absorption Analysis of CuO Nanoparticles. *Indian Journal of Advances in Chemical Science*, *2*(2), 158–161.

26. Rehana, D., Mahendiran, D., Kumar, R. S., & Rahiman, A. K. (2017). Evaluation of antioxidant and anticancer activity of copper oxide nanoparticles synthesized using medicinally important plant extracts. *Biomedicine and Pharmacotherapy*, *89*, 1067–1077.

27. Roseline, V. P., & Priya, V. (2023). Antidiabetic Potential of Copper Oxide Nanoparticles Using Biological and Polymer Functionalized Method Mediated by Sarcostemma acidum Stem Extract. *Oriental Journal Of Chemistry*, *39*(2), 387–392.

28. Selvaraj, S. P. (2022). Materials Today : Proceedings Enhanced surface morphology of copper oxide (CuO) nanoparticles and its antibacterial activities. *Materials Today: Proceedings*, *50*, 2865–2868.

29. Sharma, P., Pant, S., Poonia, P., Kumari, S., Dave, V., & Sharma, S. (2018). Green Synthesis of Colloidal Copper Nanoparticles Capped with Tinospora cordifolia and Its Application in Catalytic Degradation in Textile Dye: An Ecologically Sound Approach. *Journal of Inorganic and Organometallic Polymers and Materials*, *28*(6), 2463–2472.

30. Shehab, W. S., Elsayed, D. A., Abdel Hamid, A. M., Assy, M. G., Mouneir, S. M., Hamed, E. O., Mousa, S. M., & El-Bassyouni, G. T. (2024). CuO nanoparticles for green synthesis of significant anti-Helicobacter pylori compounds with in silico studies. *Scientific Reports*, *14*(1), 1–19.

31. Sundararaman, S. A., & Odom John, A. R. (2022). Prevention of malaria in pregnancy: The threat of sulfadoxine-pyrimethamine resistance. *Frontiers in Pediatrics*, *10*(1).

32. Tadesse, Y., & Guesh, F. (2024). Green and cost-effective biofabrication of copper oxide nanoparticles : Exploring antimicrobial and anticancer applications. *Biotechnology Reports*, *41*(December 2023), e00828.

33. Teklu, B., Kadiri, S. K., & Vidavalur, S. (2023). Green synthesis of copper oxide nanoparticles using Balanites aegyptiaca stem bark extract and investigation of antibacterial activity. *Results in Chemistry*, *6*(October), 101152.

34. Yasri, S., & Wiwanitkit, V. (2021). Artemisinin resistance: an important emerging clinical problem in tropical medicine. *International Journal of Physiology, Pathophysiology and Pharmacology*, *13*(6), 152–157.

35. Yedurkar, S. M., Maurya, C. B., & Mahanwar, P. A. (2020). Review Article Synthesis of CuO Nanoparticles Using Aloe Vera Leaf Extract and its Cytotoxic Effects on Human Carcinoma Cells. *Current Research in Green and Sustainable Chemistry*, *5*(1), 1–8.

AJBCPS African Journal of Biological, Chemical and Physical Sciences